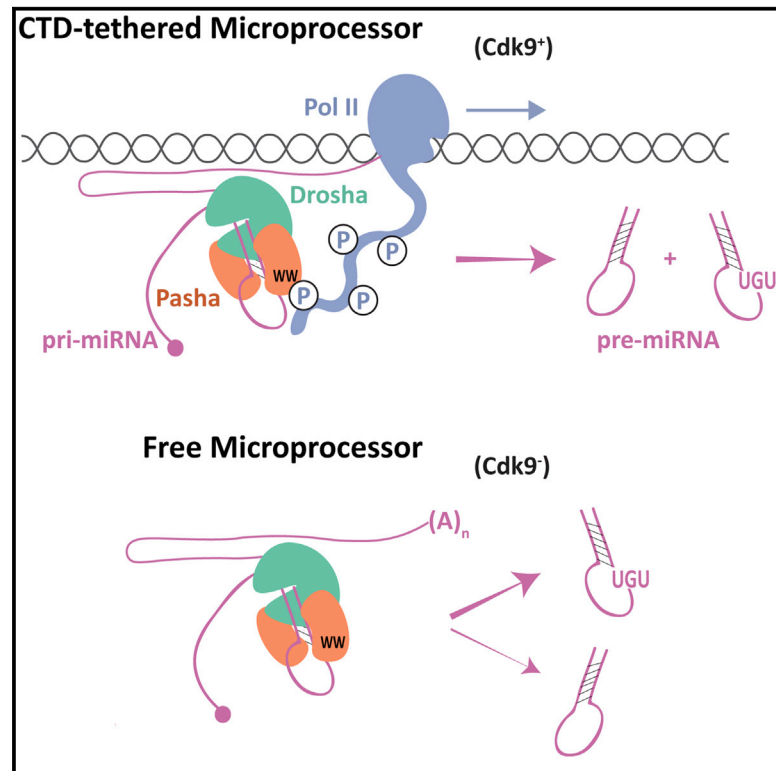


Microprocessor Recruitment to Elongating RNA Polymerase II Is Required for Differential Expression of MicroRNAs

Graphical Abstract



Authors

Victoria A. Church, Sigal Pressman, Mamiko Isaji, ..., Stephen Buratowski, Maxim V. Frolov, Richard W. Carthew

Correspondence

r-carthew@northwestern.edu

In Brief

Nuclear processing of microRNAs is a major determinant of cellular abundance of these RNAs. Church et al. find that the DGCR8 subunit of Microprocessor binds to RNA polymerase II. This couples microRNA processing to transcription. If microRNAs lack a sequence motif, co-transcriptional processing plays a more important role in determining abundance.

Highlights

- Differential nuclear processing of microRNAs affects microRNA abundance
- Microprocessor subunit DGCR8 binds to the CTD of elongating Pol II
- Co-transcriptional processing targets microRNAs lacking a UGU motif



Microprocessor Recruitment to Elongating RNA Polymerase II Is Required for Differential Expression of MicroRNAs

Victoria A. Church,¹ Sigal Pressman,¹ Mamiko Isaji,¹ Mary Truscott,² Nihal Terzi Cizmecioglu,^{3,4} Stephen Buratowski,³ Maxim V. Frolov,² and Richard W. Carthew^{1,5,*}

¹Department of Molecular Biosciences, Northwestern University, Evanston, IL 60208, USA

²Department of Biochemistry and Molecular Genetics, University of Illinois, Chicago, IL 60607, USA

³Department of Biological Chemistry and Molecular Pharmacology, Harvard Medical School, Boston, MA 02115, USA

⁴Middle East Technical University, Department of Biological Sciences, 06800, Ankara, Turkey

⁵Lead Contact

*Correspondence: r-carthew@northwestern.edu

<http://dx.doi.org/10.1016/j.celrep.2017.09.010>

SUMMARY

The cellular abundance of mature microRNAs (miRNAs) is dictated by the efficiency of nuclear processing of primary miRNA transcripts (pri-miRNAs) into pre-miRNA intermediates. The Microprocessor complex of Drosha and DGCR8 carries this out, but it has been unclear what controls Microprocessor's differential processing of various pri-miRNAs. Here, we show that *Drosophila* DGCR8 (Pasha) directly associates with the C-terminal domain of the RNA polymerase II elongation complex when it is phosphorylated by the Cdk9 kinase (pTEFb). When association is blocked by loss of Cdk9 activity, a global change in pri-miRNA processing is detected. Processing of pri-miRNAs with a UGU sequence motif in their apical junction domain increases, while processing of pri-miRNAs lacking this motif decreases. Therefore, phosphorylation of RNA polymerase II recruits Microprocessor for co-transcriptional processing of non-UGU pri-miRNAs that would otherwise be poorly processed. In contrast, UGU-positive pri-miRNAs are robustly processed by Microprocessor independent of RNA polymerase association.

INTRODUCTION

MicroRNAs (miRNAs) are a class of small non-coding RNAs that negatively regulate expression of most protein-coding genes (Bartel, 2009). They play integral roles in a variety of cellular, developmental, and physiological processes in animals (Bushati and Cohen, 2007). It is therefore important to understand how the expression levels of miRNAs are determined within cells.

Biogenesis of miRNAs begins in the nucleus with the synthesis of a capped and polyadenylated primary miRNA (pri-miRNA) transcript by RNA polymerase II (Pol II) (Cai et al., 2004; Lee et al., 2004). Embedded within a single pri-miRNA transcript are one or more hairpins of a defined structure. Each hairpin

stem is 33–35 bp in length with a terminal loop of variable size, and the hairpin is flanked by unstructured single-stranded RNA (Han et al., 2006; Lee et al., 2003; Zeng and Cullen, 2003). The Microprocessor complex, composed of the RNase III enzyme Drosha and its cofactor DGCR8, binds to these hairpins and cleaves them from pri-miRNA transcripts (Denli et al., 2004; Gregory et al., 2004; Han et al., 2004; Landthaler et al., 2004; Lee et al., 2003; Nguyen et al., 2015).

It has been found that pri-miRNA processing is more important than pri-miRNA transcription in determining the steady-state abundance of mature miRNAs within HeLa cells (Conrad et al., 2014). Moreover, pri-miRNAs often undergo differential processing. This can be inferred by the differential abundance of discrete miRNAs that are processed from a common pri-miRNA (Chaulk et al., 2011). Often, such polycistronic miRNAs show expression polarity, with the 5'-most miRNA being more abundant than downstream 3' miRNAs, even though all of the miRNAs originate from a common transcript (Conrad et al., 2014; Pfeffer et al., 2004; Yu et al., 2006). The specific ratios of these polycistronic miRNAs are often functionally important, and perturbing them results in misregulation of the cellular processes that the cluster regulates. This is associated with diseases such as cancer (Olive et al., 2013).

The mechanisms underlying differential processing of pri-miRNAs are not thoroughly understood. Processing can be controlled by RNA-binding proteins that selectively interact with certain pri-miRNAs and/or with Microprocessor (reviewed in Ha and Kim, 2014). Another mechanism controls Microprocessor processing on the basis of intrinsic structural features of the pri-miRNA itself. For example, in vitro processing activity can be enhanced or repressed by local structural features of the pri-miRNA hairpin and flanking sequences (Alarcón et al., 2015; Auyeung et al., 2013; Fang and Bartel, 2015; Han et al., 2006; Ma et al., 2013; Nguyen et al., 2015). Another potential mechanism for differential processing is that differences in miRNA levels are attributable to co-transcriptional processing of hairpins on nascent transcripts. Indeed, evidence suggests that co-transcriptional pri-miRNA processing can occur (Morlando et al., 2008; Nojima et al., 2015; Pawlicki and Steitz, 2008; Suzuki et al., 2017; Van Wynsberghe et al., 2011; Yin et al., 2015).



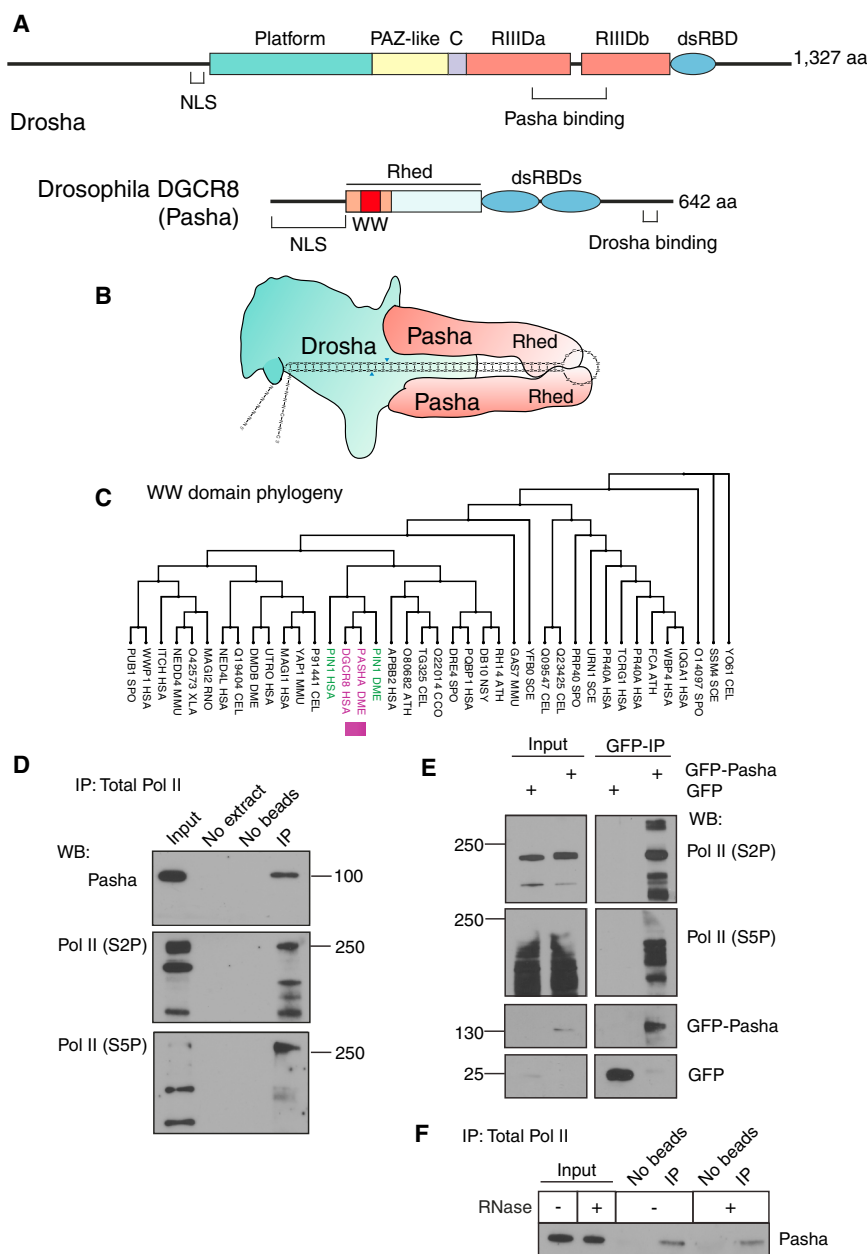


Figure 1. The Pasha Subunit of Microprocessor Associates with Phosphorylated Pol II

(A) Schematic structures of the *Drosophila* Microprocessor subunits, Drosha and Pasha. Both proteins have nuclear localization sequences (NLS). Drosha has two RNase III domains, RIIIda and RIIIdb, and a double-strand RNA-binding domain (dsRBD). Pasha has two dsRBDs and a Rhed domain, which drives homotypic dimerization and also binds heme and pri-miRNA hairpins. The WW domain is located within a region (orange) of Rhed that is sufficient for heme binding and dimerization.

(B) Model of Microprocessor structure when bound to a pri-miRNA hairpin. The cleavage site in the hairpin is marked by blue arrowheads. The model is adapted from Kim and colleagues (Kwon et al., 2016; Nguyen et al., 2015).

(C) Phylogenetic tree of a subset of eukaryotic WW domains. The sub-lineage containing DGCR8 and Pin1 is highlighted.

(D) Immunoprecipitation from S2 cell lysate using 4H8 antibody, which recognizes all CTD isoforms of Pol II (Brodsky et al., 2005; Schröder et al., 2013). Molecular weights of standards are shown on the right; 0.3% input was loaded for Pasha and 10% input for Pol II.

(E) Immunoprecipitation from S2 cell lysate using anti-GFP to purify GFP-Pasha or GFP. Molecular weights of standards are shown on the left; 2% input was loaded for Pol II, and 8% input was loaded for GFP and GFP-Pasha.

(F) Immunoprecipitation from S2 cell lysate using an antibody recognizing all Pol II isoforms (4H8), in which some samples were treated with a mixture of RNases. Precipitates were probed for Pasha as shown. 0.3% input was loaded. See also Figure S1.

hairpin, with Drosha covering the basal part of the hairpin and the two DGCR8 subunits covering the apical part (Figure 1B) (Kwon et al., 2016). On the basis of biochemical experiments, it is likely that the dimerized Rhed domains bind to apical junction and terminal loop RNA (Nguyen et al., 2015).

The domain organization of Drosha and DGCR8 proteins is strongly conserved throughout the animal kingdom (Figure 1A). Drosha has two RNase III domains, which carry out cleavage of the pri-miRNA hairpin (Han et al., 2004). The RNase domains also bind to the C-terminal tails of two DGCR8 polypeptides (Kwon et al., 2016). This generates a heterotrimeric Microprocessor complex composed of one Drosha subunit and two DGCR8 subunits (Figure 1B). The complex is further stabilized by DGCR8 homo-dimerization mediated by its Rhed domain (Quick-Cleveland et al., 2014; Weitz et al., 2014). The dimerized Rhed domain also binds to a molecule of ferric heme. Structural modeling predicts that the Microprocessor complex extends the entire length of a pri-miRNA

Embedded within the Rhed domain is a conserved WW domain whose function is currently unknown (Figures 1A and S1A). WW domains are 30–40 amino acids in length, and they mediate interactions with short proline-rich motifs in other proteins (Macias et al., 2002). To uncover a role for the DGCR8 WW domain, we performed phylogenetic analysis of the eukaryotic WW domain family. Intriguingly, DGCR8’s WW domain is most highly related to a WW domain that mediates specific binding of the Pin1 protein to the phosphorylated C-terminal domain (CTD) of the Pol II subunit Rpb1 (Figure 1C) (Morris et al., 1999; Verdecia et al., 2000). The CTD is composed of a heptad sequence YSPTSPS that is repeated 52 times in human Pol II (Jeronimo et al., 2016). It is extensively modified

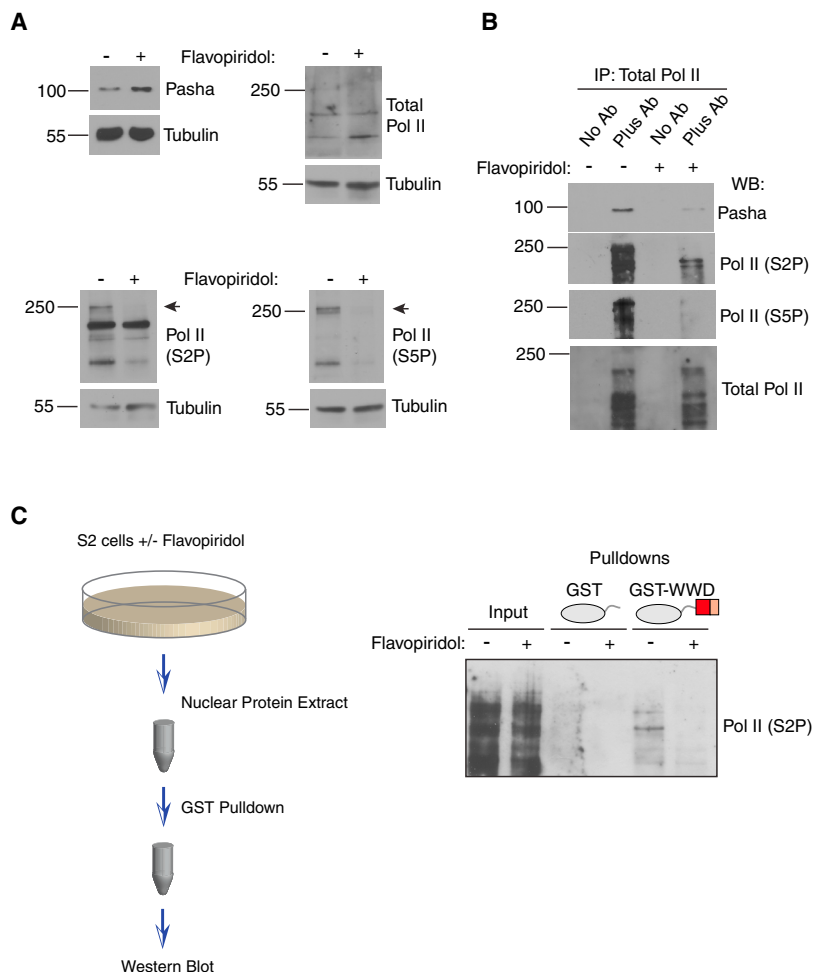


Figure 3. Pasha Binding to Pol II Requires Cdk9 Activity

(A) S2 cells were treated with flavopiridol for 20 hr. Whole-cell extracts prepared from cells were blotted for Pasha, total Pol II, S2P-modified Pol II, S5P-modified Pol II, and tubulin. (B) Extracts analyzed in (A) were subjected to immunoprecipitation with antibody specific for all isoforms of Pol II. Immunoprecipitates were probed for Pasha, total Pol II, S2P-modified Pol II, and S5P-modified Pol II. (C) S2 cells were treated with flavopiridol for 2 hr. Nuclear extracts were subjected to pull-down reactions with GST proteins, as indicated, and pulled-down material was probed for S2P-modified Pol II. Inputs represent 5% of total pull-down reactions. See also [Figure S1](#).

erased in two phases; first, shortly after initiation and second, when Pol II reaches the 3' end of the gene. In *Drosophila*, the S2 residue is phosphorylated by two kinases. Cdk9 is a subunit of pTEFb, and it phosphorylates S2 residues in Pol II situated at the 5' end of genes ([Price, 2000](#)). Cdk12 phosphorylates S2 residues in Pol II situated in the middle and at the 3' end of genes ([Bartkowiak et al., 2010](#)).

To test if the interaction between Pasha and Pol II requires CTD phosphorylation in vivo, we treated *Drosophila* S2 cells with flavopiridol, a small-molecule inhibitor of Cdk activity. At the dose applied to cells, Cdk9 was predicted to be strongly inhibited by flavopiridol, while other Cdks were less affected ([Ni et al., 2004](#)). Although 20 hr of flavopiridol treatment

repeats of the canonical CTD heptad sequence, and complexes were pulled down using streptavidin beads. Neither GST-WW nor GST-WWD formed stable complexes with peptides that were unmodified by phosphorylation ([Figures 2C and 2D](#)). In contrast, both proteins formed stable complexes with peptides that were either singly or doubly phosphorylated at the S2 and S5 positions. The K_d for binding was estimated to be approximately 4 μ M (see [Experimental Procedures](#)). To ensure that binding was not simply due to electrostatic interactions with phosphate-laden peptide, we performed the binding reaction in phosphate buffer, which competes for such electrostatic interactions ([Kim et al., 2004](#)). Specific binding to peptide with S2P was still detected ([Figure S1B](#)). Altogether, these results indicate that Pasha directly binds to the phosphorylated CTD of Pol II and that Pasha's WW domain is sufficient for the interaction to occur.

Interaction between Pasha and Pol II Requires the Cdk9 Kinase

Pol II CTD phosphorylation depends upon several serine-threonine kinases ([Buratowski, 2009](#); [Jeronimo et al., 2016](#)). Cdk7 is a subunit of TFIIF, and it phosphorylates S5 and S7 in the CTD repeat. This occurs in the pre-initiation complex and is thought to aid in promoter escape and pausing by Pol II. The marks are

strongly inhibited Pol II phosphorylation, it had no effect on total Pol II and Pasha protein levels ([Figure 3A](#)). We then immunoprecipitated all Pol II isoforms and determined that co-immunoprecipitation of Pasha was greatly reduced in the flavopiridol-treated samples ([Figure 3B](#)). As expected, little or no S2P- or S5P-modified Pol II was immunoprecipitated from these samples. We next prepared nuclear extracts from cells treated for 2 hr with flavopiridol. Because Pol II must be completely dephosphorylated before flavopiridol can have an effect on its phosphorylation state, 2 hr was not long enough for many Pol II molecules to go through a dephosphorylation-phosphorylation cycle. Extracts were incubated with GST-WWD protein, which was used to pull down newly associated complexes. A physical interaction between GST-WWD and S2P-modified Pol II was strongly inhibited in extracts from flavopiridol-treated cells ([Figures 3C and S1C](#)). Thus, de novo binding of added GST-WWD protein appeared to be highly specific for newly phosphorylated Pol II. The newly phosphorylated molecules might not be masked by interacting nuclear factors and thus are more free to associate with the exogenous bait protein. In summary, dynamic phosphorylation of Pol II by Cdk9, and possibly other Cdks, is necessary for the in vitro and in vivo association of Pasha and Pol II.

Cdk9 Activity Regulates miRNA Levels In Vivo

We asked whether the Pasha-Pol II interaction has a functional impact on Microprocessor activity. Point mutations in the WW domain of DGCR8 that potentially would disrupt Pol II binding result in impaired dimerization or heme binding, both of which lead to insoluble protein (Quick-Cleveland et al., 2014). Homologous mutations in Pasha also caused protein insolubility (data not shown). Therefore, we could not generate *cis*-mutations that would specifically block Pol II binding. Instead, we reasoned that loss of Cdk9 would affect Microprocessor activity if there was such a functional connection, because loss of Cdk9 activity impairs the physical association between the proteins. We isolated a mutant strain of *Drosophila* that had a point mutation in the *cdk9* gene. The point mutation results in a single amino acid substitution of the first invariant glycine in the ATP-binding motif GXGXXG located in the kinase domain (Figure S2A). The G57S mutant allele is homozygous lethal, and mutant larvae arrest their development at the L1-L2 transition before dying (Figures S2B and S2C). To demonstrate that the mutation was responsible for the lethal phenotype, we created a *Cdk9* transgene (Figure S2D). The transgene fully rescued the lethal mutant phenotype, and a single transgene copy was sufficient to rescue the developmental defects (Figure S2E) and produce fertile adult flies (data not shown). Although the mutant is organismal lethal, it is not cell lethal (Figure S2F).

We tested the mutant for its effect on S2 and S5 phosphorylation of Pol II. Western analysis of Pol II from mutant animals showed that Pol II protein levels were normal, but S2P- and S5P-modified Pol II levels were strongly inhibited (Figures 4A and S3A). Thus, S2 and S5 phosphorylation is strongly dependent upon Cdk9 activity in vivo. Although Cdk7 and Cdk12 have been found to contribute to CTD phosphorylation in *Drosophila* (Barkowiak et al., 2010; Schwartz et al., 2003), Cdk9 may provide phospho-marks on elongating Pol II, with the other kinases transiently marking initiating and terminating Pol II complexes. We attempted to perform Pasha-Pol II co-immunoprecipitations in extracts derived from the mutant larvae, but non-specific proteolysis in these extracts precluded their completion (data not shown).

If Cdk9 regulates Microprocessor activity, we reasoned that the *cdk9* mutant would have abnormal levels of processed miRNAs. Therefore, we performed small-RNA sequencing on homozygous wild-type and mutant larvae collected at the L1-L2 transition (Table S1). This time point was chosen because it was close to the lethal phase, but the mutant animals were still developmentally synchronized with the wild-type animals. Thus, any differences in miRNA levels between mutant and wild-type would not be due to asynchronous development. As a further effort to exclude mutant effects unrelated to processing, we first considered pri-miRNA transcripts that contain more than one hairpin, and individually generate multiple miRNAs. If Cdk9 had differential effects on polycistronic miRNAs originating from the same pri-miRNA transcript, this would suggest that processing was affected.

Five loci were predicted to encode polycistronic miRNAs that were detected in the sequenced libraries (Figure 4B) (Ryazansky et al., 2011; Sun et al., 2015; Truscott et al., 2011). Using nested RT-PCR and 3'RACE, we validated that all five loci generate pri-

miRNAs encompassing the relevant miRNAs; that is, the pri-miRNAs are polycistronic in L1 larvae (Figures S3B–S3D). Examination of the sequencing data found that three of the five clusters exhibited an expression polarity such that the 5'-most mature miRNA was more abundant than the 3' mature miRNAs derived from the same cluster (Figure 4C). Strikingly, this expression polarity was impaired in the *cdk9* mutant for all three clusters (Figures 4C and 4D). Abundance of the 5'-most miRNA was reduced, while 3' miRNAs either increased in abundance or remained constant. We also observed differences with the other two clusters. The miR-279/996 cluster exhibited the opposite polarity in wild-type animals, with the 3'-most miR-996 being more abundant than miR-279. However, approximately equal levels of miR-279 and miR-996 were detected in the *cdk9* mutant (Figure 4C). The fifth miRNA cluster was unique in that the two hairpins encoding miR-275 and miR-305 are spaced only 80 bp apart, significantly less than the 500 or more base pairs that exist between hairpins in the other clusters (Figure 4B). Interestingly, miR-275 and miR-305 are expressed at equivalent levels in wild-type, but the 3' miR-305 is almost exclusively expressed in the mutant (Figure 4C). We validated the results of RNA-seq analysis by independently measuring levels of the more abundant miRNAs in wild-type and mutant, using a splinted-ligation assay (Maroney et al., 2007) (Figure S4A). Thus, Cdk9 affects differential abundance of miRNAs originating from common precursor RNAs.

One possible reason for the differential effect is that Cdk9 affects pri-miRNA synthesis, and therefore pri-miRNA levels change in the mutant in concordance with altered mature miRNA levels. To test this possibility, we performed RT-qPCR on pri-miRNA transcripts. To ensure that our RT-qPCR analysis was measuring bona fide pri-miRNAs, we measured RNA levels in a *droscha* mutant (Figure S4B). Because Droscha is essential for pri-miRNA processing, its loss should increase abundance of the pri-miRNA precursors. Indeed, most probes measured higher levels of mutant RNA, consistent with their detection of pri-miRNAs. We then compared pri-miRNA levels between *cdk9* mutant and wild-type animals (Figure 4E). The miR-279/-996 pri-miRNA was increased in the *cdk9* mutant, suggesting an effect on processing. Three of five clusters showed no significant change in pri-miRNA levels in the *cdk9* mutant. The reason why the mutant did not elicit a significant change in these pri-miRNA levels is likely because the mature miRNA levels are only reduced 1.5- to 3-fold in the mutant relative to wild-type, in contrast to the *droscha* mutant, which had a greater effect because processing was abolished. The miR-275/-305 pri-miRNA was reduced in the mutant, whereas the level of mature miR-305 was increased, suggesting an effect on processing and not synthesis. Overall, these results indicate that altered miRNA levels cannot be explained by an effect of Cdk9 on pri-miRNA synthesis.

An Apical Junction Motif in pri-miRNA Hairpins Is Related to Differential Processing

Sequence motifs in the pri-miRNA hairpin ensure accurate and efficient pri-miRNA processing in vitro (Auyeung et al., 2013; Fang and Bartel, 2015; Ma et al., 2013; Nguyen et al., 2015). These determinants include an apical junction motif composed

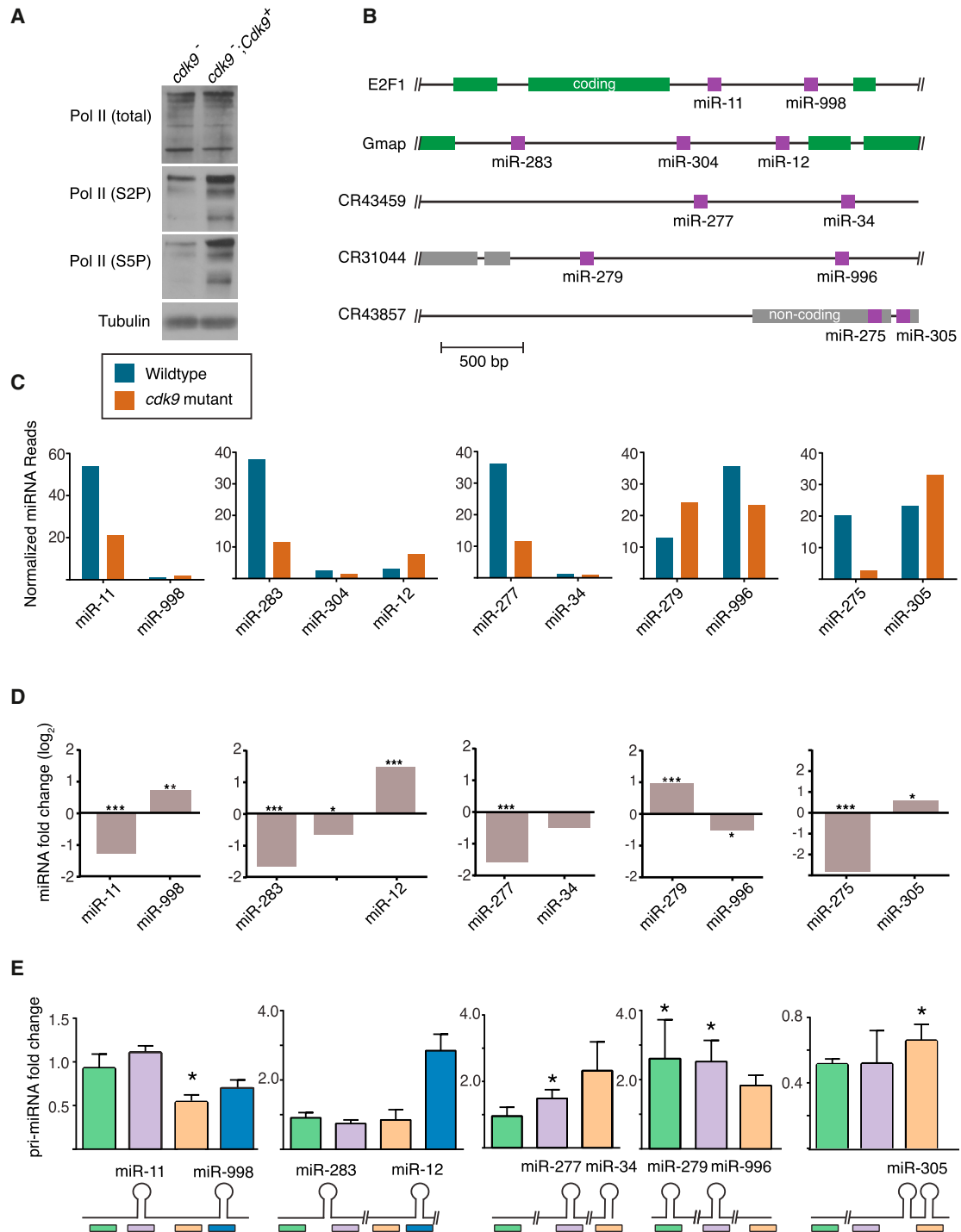


Figure 4. *Cdk9* Is Required for Differential miRNA Processing

(A) Western blot of total Pol II and specific phospho-isoforms of Pol II from *cdk9* mutant tissue.

(B) Schematic structures of five polycistronic genes that were analyzed for miRNA expression.

(C) Levels of mature miRNAs expressed from polycistronic genes. Shown are normalized RNA-seq read levels (1,000s) from animals that are wild-type and *cdk9* mutant.

(D) Differential expression of mature miRNAs between mutant and wild-type animals as determined by RNA-seq. * $p \leq 0.01$, ** $p \leq 0.001$, and *** $p \leq 0.0001$ (edgeR exact test).

(E) Differential expression of pri-miRNAs between mutant and wild-type animals as determined by RT-qPCR. Shown below are positions of the various RT-qPCR products being assayed. Error bars represent SD. * $p \leq 0.01$ (t test).

See also Figure S2.

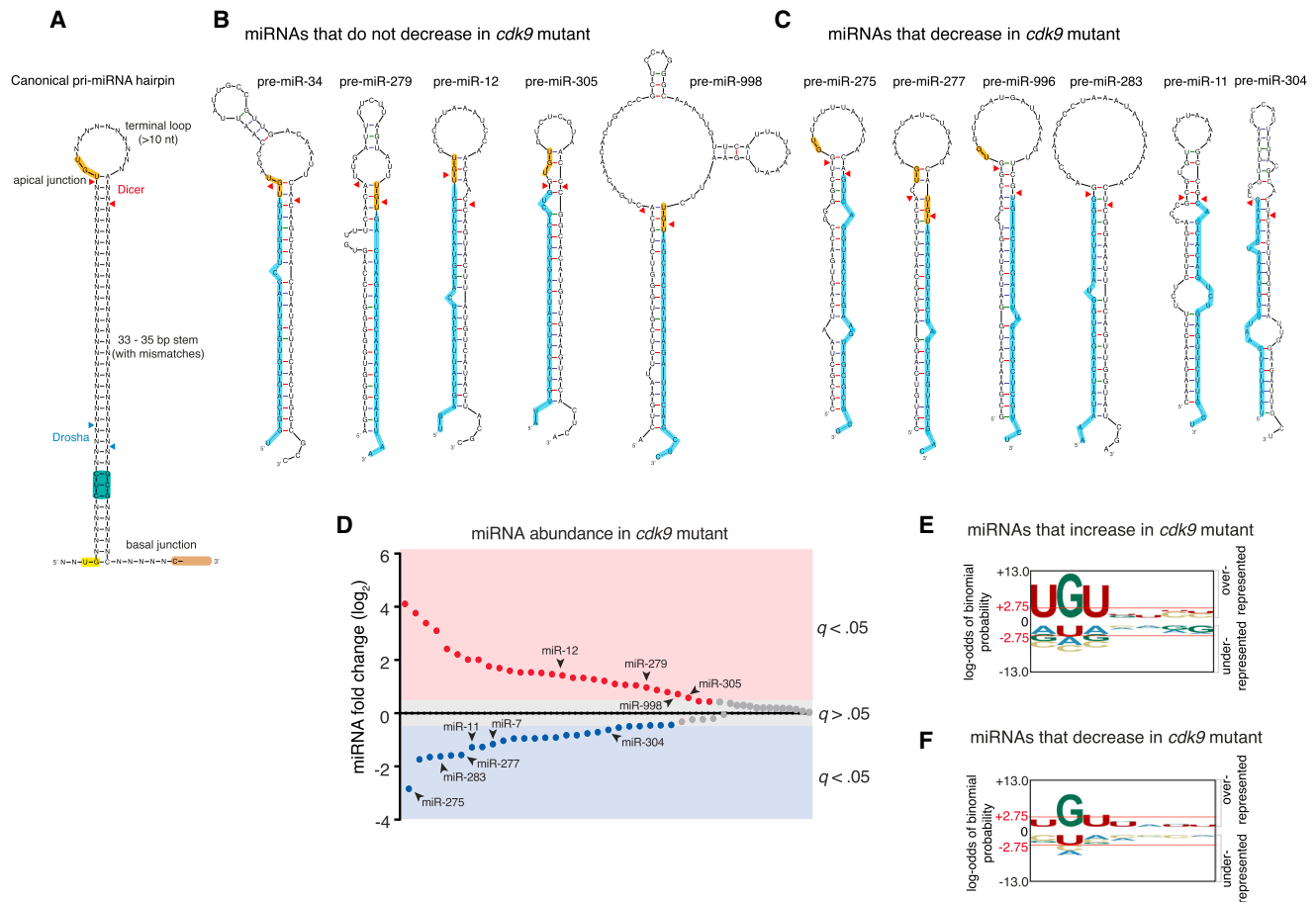


Figure 5. An Apical Junction Sequence Is Related to Cdk9-Dependent Processing

(A) Generalized structural and sequence features of pri-miRNA hairpin. Sequence motifs that affect *in vitro* processing specificity and efficiency are highlighted. Cleavage sites for Drosha and Dicer are shown with arrowheads.

(B) Predicted pre-miRNA structures for those miRNAs whose abundance did not decrease in *cdk9* mutants. Highlighted are the UGU motif (yellow) and mature miRNA (blue).

(C) Predicted pre-miRNA structures for those miRNAs whose abundance decreased in *cdk9* mutants. For (B) and (C), mFold and RNAfold were independently used to predict the pre-miRNA structures.

(D) Differential expression of all miRNAs detected by RNA-seq between mutant and wild-type samples. miRNAs are ranked by fold change, and those whose fold change is considered significant (FDR below 5%) are colored. Those miRNAs that are derived from polycistronic genes are noted.

(E and F) Logo graphs of nucleotide sequence bias within the apical junctions of pri-miRNA hairpins. Contrasted are the 30 miRNAs whose expression is greater in *cdk9* mutants (E) versus the 26 miRNAs whose expression is reduced in *cdk9* mutants (F). The y axes correspond to the binomial probability of residue frequencies, with respect to the background of all *Drosophila* pre-miRNA sequences. Threshold values of $p < 0.05$ significance (2.75) are shown in red and marked with red horizontal lines.

See also Figures S3 and S4.

of UGU and two basal junction motifs: UG and CNNC (Figure 5A). They enhance *in vitro* processing but are not essential. We wondered whether these motifs or some unknown sequence motif might be related to the differential processing regulated by Cdk9. Therefore, we analyzed polycistronic miRNA hairpin sequences that were affected by the *cdk9* mutant. The only motif that showed hints of a correlation was the apical junction UGU. miRNAs that did not decrease in *cdk9* mutants typically contained a UGU in their apical junctions (Figure 5B), whereas those that decreased in *cdk9* mutants did not have a UGU (Figure 5C). Although this might suggest that presence of a UGU

motif in hairpins is related to differential processing events mediated by Cdk9, the number of hairpins was too small to make any definite conclusion. However, the polycistronic miRNAs we examined represent only a small fraction of the miRNAs that were affected by the *cdk9* mutant. In total, out of 77 miRNAs detected (Table S1), 30 miRNAs were significantly overexpressed in *cdk9* mutants, while 26 miRNAs were under-expressed (Figure 5D). Thus, many monocistronic miRNAs were also affected by *cdk9*. To confirm that monocistronic miRNA levels were affected by *cdk9* in the same manner as polycistronic miRNAs, we examined two of the monocistronic miRNAs: miR-7 and

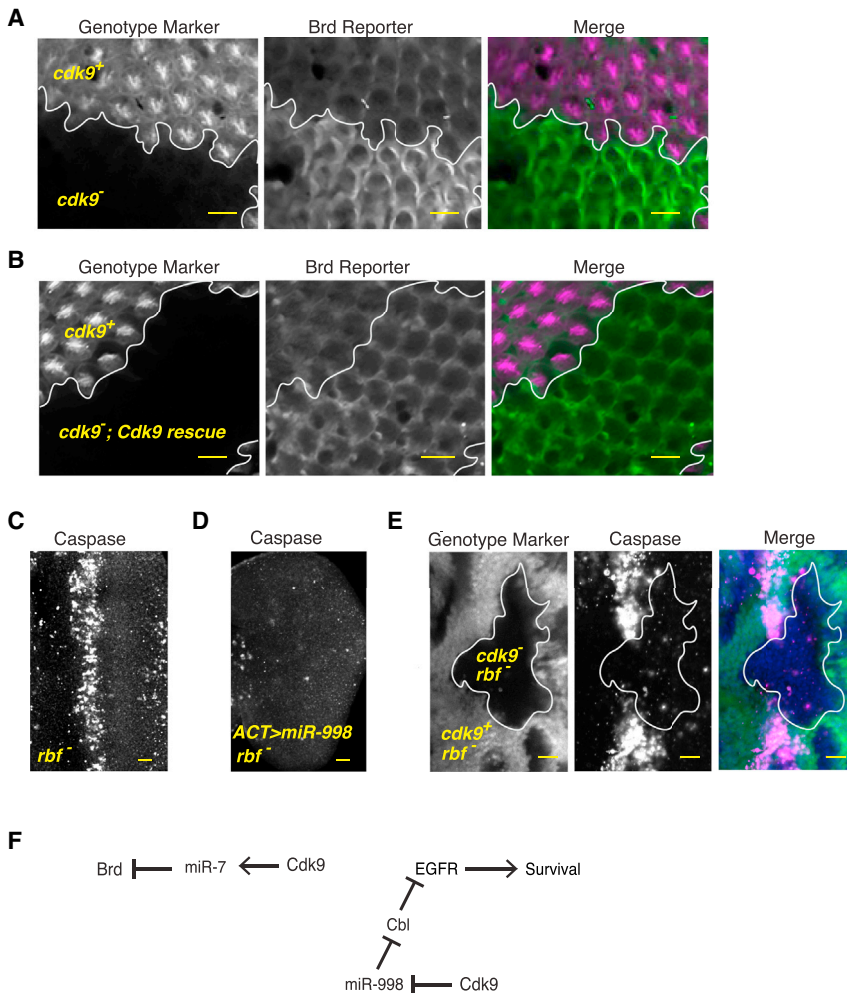


Figure 6. Differential Processing Has a Significant Effect on Gene Silencing In Vivo

(A) Expression of the *Brd* reporter gene in the developing eye. The image contains approximately 800 cells, some of which are genetically wild-type and some of which are mutant for the *cdk9* gene. Cell genotypes have been marked by the presence or absence of an RFP marker, as indicated. RFP and GFP channels are shown separately along with a merged image.

(B) The clone of mutant *cdk9* mutant cells also expressed the *Cdk9* rescue transgene, and consequently, silencing of the *Brd* reporter is restored within these cells.

(C) When *rbf* mutant eye discs are stained for activated caspase protein, they show a zone of prevalent cell apoptosis within the morphogenetic furrow. (D) This zone is absent if eye cells overexpress miR-998 via the GAL4/UAS system.

(E) When *rbf* mutant cells are also mutant for *cdk9*, there is greatly reduced apoptosis.

(F) A summary of the genetic experiments showing the pathways of gene regulation downstream of Cdk9.

Scale bars for (A)–(E) represent 10 μ m. See also Figure S5.

Cdk9 Is Required for Proper miRNA-Mediated mRNA Silencing In Vivo

Microprocessor appears to associate with Pol II, which leads to differential processing of certain pri-miRNA hairpins. Is this of functional importance? To explore the question, we looked at the effects of the *cdk9* mutant on miRNA-mediated gene regulation. We had previously generated a transgenic reporter for miRNA regulation

of the *Bearded (Brd)* gene (Pressman et al., 2012). This reporter is regulated by miR-7, which is reduced in the *cdk9* mutant (Figure S5A). Therefore, we assayed the reporter in a developing eye that contained clones of *cdk9* mutant cells (Figure 6A). Mutant cells showed a dramatic upregulation of reporter expression. If *cdk9* mutant eye clones also contained the *Cdk9* rescue transgene, reporter expression was not upregulated to the same degree (Figure 6B). Reporter mRNA abundance and structure were unchanged in the mutant, as demonstrated by 3'-RACE (Figure S5B). These results indicate that miR-7-mediated *Brd* gene regulation is impaired in *cdk9* mutant cells.

Other miRNAs are overexpressed in the *cdk9* mutant, including miR-998. This miRNA has an anti-apoptotic function in the developing eye, where it enhances survival signaling via EGFR (Truscott et al., 2014). MiR-998 does so by directly repressing *Cbl*, a negative regulator of EGFR signaling. Anti-apoptotic function of miR-998 was studied in the context of an *rbf* mutation, which induces a high level of apoptosis (Figure 6C). If miR-998 is overexpressed, apoptosis is completely blocked (Figure 6D). We reasoned that because *cdk9* mutant cells overexpressed miR-998, this might also be sufficient to block apoptosis in the eye. Therefore, we generated clones of *cdk9*

of the *Bearded (Brd)* gene (Pressman et al., 2012). This reporter is regulated by miR-7, which is reduced in the *cdk9* mutant (Figure S5A). Therefore, we assayed the reporter in a developing eye that contained clones of *cdk9* mutant cells (Figure 6A). Mutant cells showed a dramatic upregulation of reporter expression. If *cdk9* mutant eye clones also contained the *Cdk9* rescue transgene, reporter expression was not upregulated to the same degree (Figure 6B). Reporter mRNA abundance and structure were unchanged in the mutant, as demonstrated by 3'-RACE (Figure S5B). These results indicate that miR-7-mediated *Brd* gene regulation is impaired in *cdk9* mutant cells.

Other miRNAs are overexpressed in the *cdk9* mutant, including miR-998. This miRNA has an anti-apoptotic function in the developing eye, where it enhances survival signaling via EGFR (Truscott et al., 2014). MiR-998 does so by directly repressing *Cbl*, a negative regulator of EGFR signaling. Anti-apoptotic function of miR-998 was studied in the context of an *rbf* mutation, which induces a high level of apoptosis (Figure 6C). If miR-998 is overexpressed, apoptosis is completely blocked (Figure 6D). We reasoned that because *cdk9* mutant cells overexpressed miR-998, this might also be sufficient to block apoptosis in the eye. Therefore, we generated clones of *cdk9*

mutant cells in the *rbf* eye and found that these cells, like cells overexpressing miR-998, were completely protected from apoptosis (Figure 6E). In summary, Cdk9 is required for generating levels of miRNAs appropriate for regulating normal cellular functions (Figure 6F).

DISCUSSION

We provide evidence for a direct interaction between a component of the Microprocessor complex and Pol II. Our results are consistent with previous studies suggesting that select miRNAs are co-transcriptionally processed and that co-transcriptional processing is specifically associated with CTD-phosphorylated Pol II (Morlando et al., 2008; Nojima et al., 2015; Pawlicki and Steitz, 2008). Our results are also consistent with Drosha association with Pol II and ChIP detection of DGCR8 at pri-miRNA loci in a variety of cells (Gromak et al., 2013; Suzuki et al., 2017). We found that Cdk9 stimulates processing of miRNAs that lack a UGU apical junction motif, whereas miRNAs that contain a UGU motif are not stimulated by Cdk9. From in vitro studies, it was found that a pri-miRNA is processed by purified Microprocessor more efficiently if the pri-miRNA has a UGU motif (Nguyen et al., 2015). However, if DGCR8 lacks its Rhed domain, the UGU motif has no effect on processing efficiency. This indicates that the Rhed domain is essential for freely diffusing Microprocessor to functionally interact with the UGU motif. It is also consistent with binding studies that find the Rhed domain physically associates with the apical junction (Nguyen et al., 2015; Quick-Cleveland et al., 2014).

How then does Pol II association stimulate the processing of UGU-negative miRNAs but not UGU-positive miRNAs? One model is that when bound to Pol II, Microprocessor alters its intrinsic preference for RNA processing on the basis of the UGU motif. Another model is that tethering of Microprocessor to Pol II does not affect its intrinsic processing activity. Instead, tethering increases the effective concentration of Microprocessor at the site of hairpin RNA synthesis, consequently enhancing the rate of co-transcriptional processing. The latter model is favored by in vitro processing studies. When phosphorylated peptide is added to in vitro Microprocessor reactions, the peptide has no effect on pri-miRNA processing efficiency, regardless of whether the substrate RNA contains a UGU motif or not (N. Kim and T.A. Nguyen, personal communication). Although the model would predict that tethering stimulates UGU and non-UGU RNA substrates equally, this is not seen. Possibly when tethering is lost, UGU-containing RNA substrates are still efficiently processed in the nucleoplasm. However, because non-UGU substrates are processed so inefficiently as free entities, the bulk of their processing would instead be achieved by tethering Microprocessor to Pol II and localizing it near nascent pri-miRNA transcripts. This would make non-UGU substrates more dependent upon tethering. To summarize, pri-miRNA processing is accelerated by either the presence of a UGU motif in the RNA substrate or by tethering of Microprocessor. In diverse animal species, only one-third of pri-miRNA hairpins contain a UGU motif, suggesting that these two mechanisms might be an important and conserved feature of differential pri-miRNA processing.

The most parsimonious mechanism to account for the results of our study and other studies is that the Pasha-Pol II interaction directly mediates differential processing. If so, then a *cis*-mutation in Pasha's WW domain that blocks Pol II interaction would phenocopy the processing defects of the *cdk9* mutant. However, a systematic mutation of the Pasha WWD domain was unsuccessful because proteins were insoluble (data not shown). Therefore, it remains a formal possibility that the Cdk9 effect on processing is indirect. However, we found that Cdk9-dependent processing is strongly related to the UGU motif in the apical junction of the pre-miRNA precursor, which directly associates with the Rhed domain. If the Cdk9 effects on differential processing were indirect, it becomes difficult to parse how the presence or absence of a UGU motif relates to it.

Why are there distinct mechanisms for nuclear processing of pri-miRNAs? We do not think that these mechanisms act on miRNAs according to their expression level. Analysis of our data did not find a significant correlation between the abundance of miRNAs and either *cdk9* responsiveness or the UGU motif. Rather, we think that these mechanisms enable efficient processing of polycistronic transcripts. If only one or two Microprocessor molecules are tethered to each elongating Pol II, then tethered Microprocessor would encounter the 5' hairpins first, dissociate from Pol II, and process them. Processing of more distal miRNAs would necessitate a non-tethered mechanism, which is more efficient if the hairpins contain a UGU motif. The net result would be differential expression of miRNAs from a polycistronic transcript, which is frequently observed. There might be other reasons for processing to occur by distinct mechanisms. For hairpins embedded within introns, they would be more efficiently excised by tethered Microprocessor from nascent transcripts before splicing occurs (Pawlicki and Steitz, 2008). Indeed, intronic hairpins can be processed from unspliced introns (Kim and Kim, 2007). For hairpins that reside in exons, tethered processing might not be essential for efficient excision, and so free Microprocessor could act on them. Finally, tethered processing could be susceptible to regulatory processes distinct from processing in the free nucleoplasm. Local chromatin organization, histone modification, and the proximity of *cis*-acting RNAs and proteins might regulate Microprocessor activity when tethered to Pol II. Regulated RNA splicing is controlled by such mechanisms (Naftelberg et al., 2015), so it is plausible for pri-miRNA processing to be as well.

EXPERIMENTAL PROCEDURES

Genetics

A list of all *Drosophila* genotypes used is presented in Table S2. An EMS-mutagenesis screen previously described was used to generate the *cdk9*^{G57S} mutant strain (Pressman et al., 2012). The mutation was meiotically mapped to the *cdk9* locus, and a base substitution of G to A in the gene's coding sequence was detected. To prove that the *cdk9* mutation was responsible for the phenotypes, a 2.5 kb fragment of genomic DNA encompassing the *cdk9* gene (Figure S2) was cloned into the pYES vector (Patton et al., 1992). Transgenic lines were created using P element-mediated transformation.

Cell Culture

Drosophila S2⁺ cells were cultured in Schneider's media supplemented with 10% FBS (Invitrogen). To make stable cell lines, cells were transfected with either GFP or GFP-Pasha expressing pmK33 plasmid vectors and selected

for 4–5 weeks on Hygromycin B until > 90% cells expressed GFP or GFP-Pasha when induced with 250 μM CuSO_4 for 12–16 hr. For flavopiridol treatment, cells were plated at 2×10^6 cells/mL and treated with 0.5 μM flavopiridol (Sigma-Aldrich) for 2 or 12 hr. Longer treatments were necessary to allow sufficient induction of GFP or GFP-Pasha after addition of CuSO_4 .

Analysis of *cdk9* Mutant Larvae

Balanced *cdk9*^{G57S} animals were crossed, and progeny were collected. Balancer chromosomes carried a *twist>GFP* transgene, so after 48 hr, non-fluorescent larval progeny were isolated. They were gently washed in deionized water and either frozen or immediately extracted for RNA. RNA extraction was performed using Trizol. For western blotting, larvae were lysed in RIPA buffer (50 mM Tris-Cl [pH 7.4], 150 mM NaCl, 1 mM EDTA, 1.0% NP-40, 0.5% sodium deoxycholate, and 0.1% SDS) plus protease and phosphatase inhibitors and spun at $16,000 \times g$ for 15 min at 4°C before performing SDS-PAGE.

RNA-Seq

Small-RNA-seq libraries were prepared and sequenced on an Illumina platform as described (Gu et al., 2009; Shirayama et al., 2012). Because *Drosophila* expresses a 2S rRNA that is 30 nt in length, we size-selected RNAs between 15 and 29 nt by gel purification before library preparation. Reads were mapped to the *Drosophila* genome build dm3 using Bowtie. Annotation was performed using Avadis NGS software. Read counts were normalized by library size in EdgeR/DESEQ and the data were filtered so that only miRNAs that had 500 or more reads across samples were analyzed.

Northern Blot, Splinted Ligation, RT-qPCR, and 3'RACE

For all RNA analysis, total RNA purified by Trizol was assayed. Oligos used for RNA analysis are listed in Table S3. For northern blots, 20 μg of total RNA was electrophoresed on a 15% acrylamide/8M urea gel. Membranes were chemically cross-linked with EDC (0.15 M 1-methylimidazole, 0.16 M *N*-Ethyl-*N'*-[3-dimethylaminopropyl]carbodiimide [pH 8.0]) for 2 hr at 60°C. The membrane was then pre-hybridized in ULTRAhyb (Ambion) for 30 min at 60°C. Oligonucleotide complementary to 2S rRNA (IDT) and locked nucleic acid oligos complementary to mature miR-7 and miR-14 (Exiqon) were hybridized overnight at 37°C. Blots were washed at 37°C in 2X SSC, 0.1% SDS, and then in 0.1X SSC and 0.1% SDS.

For splinted ligation assays of mature miRNAs, reactions were carried out as described (Lee et al., 2009; Maroney et al., 2007). A ligation oligo was 5' end-labeled with [^{32}P]-ATP. The labeled product was phenol-chloroform-extracted and diluted in 100 μL RNase free H_2O . Bridge oligos were designed on the basis of the corresponding miRbase miRNA sequences. Bridge oligos were synthesized with a three-carbon spacer at the 3' end. Five to 20 μg total RNA from 48 hr *cdk9*^{G57S} and wild-type larvae was used for each ligation reaction, including T4 DNA ligase (NEB). For each assay, three negative controls were performed, leaving out ligase, RNA, or bridge oligo. Reaction products were resolved on 12% urea-polyacrylamide gels. Gels were imaged overnight on a PhosphorImager. Data were quantified in ImageQuant, and signals for each miRNA product were corrected for control backgrounds, normalized to 2S rRNA, and then reported as the \log_2 (fold change) for *cdk9*^{G57S} relative to wild-type.

For RT-qPCR, 2.5 μg of total RNA was primed with a 1:2 molar mix of oligo-dT:random 9mers for the RT reaction. qPCR was performed on a Biorad iCycler, and the delta-delta Ct method was used to measure output. Rpl32 was used to normalize RNA levels.

3'RACE and nested RT-PCR were performed using gene-specific RT primers (listed in Table S3) and Q_o , Q_i , Q_T primers (Scotti-Lavino et al., 2006). Briefly, total RNA was purified from 48 hr wild-type or *droscha*^{O884X} larvae using Trizol. Reverse transcription was performed with Superscript III using 5 μg total RNA per reaction and Q_T or R_o primers (for 3'RACE or nested PCR, respectively). cDNA reactions were treated with 0.75 μL RNase H (Promega) for 20 min at 37°C and diluted in 1 mL of TE (Tris-EDTA buffer [pH 8.0]). The first PCR round was performed with 1 μL of cDNA per 50 μL PCR reaction and the following primers: Q_o and GSP1 primers for 3'RACE or the "outer" gene specific primers for nested PCR. The second PCR round was performed with 1 μL of a 1:20 dilution of round one PCR, using Q_i and GSP2 primers for

3'RACE or the "inner" gene specific primers for nested PCR. All PCRs were performed with GoTaq DNA polymerase following the supplied protocol (Promega).

Apoptosis Assay

Eye imaginal discs were dissected from third-instar larvae in Schneider's insect medium (Sigma-Aldrich) and then fixed in PBS buffer with 4% formaldehyde. Discs were then blocked in PBS + 0.1% Triton X-100 (PBST) + 10% normal donkey serum followed by overnight incubation with rabbit anti-C3 (cleaved caspase-3), lot 26, 1:50 (Cell Signaling). Discs were washed in PBST and incubated in blocking solution containing the appropriate secondary antibodies: Cy3- or Cy5-conjugated anti-rabbit antibodies, 1:300 (Jackson ImmunoResearch). After washing in TBST, discs were placed into glycerol containing 0.5% propyl gallate in preparation for slide mounting. Imaging was performed using a Zeiss LSM Observer.Z1.

Protein Association Assays

Immunoprecipitations, GST pull-downs, and peptide binding assays were performed essentially as described (Green and Sambrook, 2012; Kim et al., 2004), with some modifications. See the Supplemental Information for precise details of these assays.

Data and Software Availability

The accession number for the RNA-seq data reported in this paper is GEO: GSE103234.

SUPPLEMENTAL INFORMATION

Supplemental Information includes Supplemental Experimental Procedures, five figures, and three tables and can be found with this article online at <http://dx.doi.org/10.1016/j.celrep.2017.09.010>.

AUTHOR CONTRIBUTIONS

Conceptualization, V.A.C., S.P., and R.W.C.; Methodology, V.A.C., S.B., M.V.F., and R.W.C.; Investigation, V.A.C., S.P., M.I., M.T. and N.T.C.; Formal Analysis, V.A.C.; Writing – Original Draft, V.A.C. and R.W.C.; Writing – Review and Editing, S.P., M.I., M.T., N.T.C., S.B., and M.V.F.; Visualization, V.A.C. and R.W.C.; Supervision, M.V.F., S.B., and R.W.C.

ACKNOWLEDGMENTS

We thank Narry Kim and Tuan Ahn Nguyen for kindly sharing their results on peptide interactions with Microprocessor activities in vitro. We thank Matt Schipma of the Northwestern Genomics Core and Weifeng Gu for assistance with RNA-seq adaptor removal and genome alignment. We also thank J. Brickner, G. Hannon, and C. Horvath for gifts of reagents. We thank G. Beitel and our lab colleagues for their advice. This work was supported by the NIH (T32GM08061 to V.A.C., R01GM110018 to M.V.F., R01GM56663 to S.B., and R01GM077581 and R35GM118144 to R.W.C.).

Received: August 24, 2016

Revised: August 18, 2017

Accepted: September 4, 2017

Published: September 26, 2017

REFERENCES

- Alarcón, C.R., Lee, H., Goodarzi, H., Halberg, N., and Tavazoie, S.F. (2015). N6-methyladenosine marks primary microRNAs for processing. *Nature* 519, 482–485.
- Auyeung, V.C., Ulitsky, I., McGeary, S.E., and Bartel, D.P. (2013). Beyond secondary structure: primary-sequence determinants license pri-miRNA hairpins for processing. *Cell* 152, 844–858.
- Bartel, D.P. (2009). MicroRNAs: target recognition and regulatory functions. *Cell* 136, 215–233.

- Bartkowiak, B., Liu, P., Phatnani, H.P., Fuda, N.J., Cooper, J.J., Price, D.H., Adelman, K., Lis, J.T., and Greenleaf, A.L. (2010). CDK12 is a transcription elongation-associated CTD kinase, the metazoan ortholog of yeast Ctk1. *Genes Dev.* **24**, 2303–2316.
- Brodsky, A.S., Meyer, C.A., Swinburne, I.A., Hall, G., Keenan, B.J., Liu, X.S., Fox, E.A., and Silver, P.A. (2005). Genomic mapping of RNA polymerase II reveals sites of co-transcriptional regulation in human cells. *Genome Biol.* **6**, R64.
- Buratowski, S. (2009). Progression through the RNA polymerase II CTD cycle. *Mol. Cell* **36**, 541–546.
- Bushati, N., and Cohen, S.M. (2007). microRNA functions. *Annu. Rev. Cell Dev. Biol.* **23**, 175–205.
- Cai, X., Hagedorn, C.H., and Cullen, B.R. (2004). Human microRNAs are processed from capped, polyadenylated transcripts that can also function as mRNAs. *RNA* **10**, 1957–1966.
- Chaulk, S.G., Thede, G.L., Kent, O.A., Xu, Z., Gesner, E.M., Veldhoen, R.A., Khanna, S.K., Goping, I.S., MacMillan, A.M., Mendell, J.T., et al. (2011). Role of pri-miRNA tertiary structure in miR-17~92 miRNA biogenesis. *RNA Biol.* **8**, 1105–1114.
- Conrad, T., Marsico, A., Gehre, M., and Orom, U.A. (2014). Microprocessor activity controls differential miRNA biogenesis in vivo. *Cell Rep.* **9**, 542–554.
- Denli, A.M., Tops, B.B., Plasterk, R.H., Ketting, R.F., and Hannon, G.J. (2004). Processing of primary microRNAs by the Microprocessor complex. *Nature* **432**, 231–235.
- Fang, W., and Bartel, D.P. (2015). The menu of features that define primary microRNAs and enable de novo design of microRNA genes. *Mol. Cell* **60**, 131–145.
- Green, M., and Sambrook, J. (2012). *Molecular Cloning: A Laboratory Manual*, 4th ed. (New York: Cold Spring Harbor Laboratory Press).
- Gregory, R.I., Yan, K.P., Amuthan, G., Chendrimada, T., Doratotaj, B., Cooch, N., and Shiekhattar, R. (2004). The Microprocessor complex mediates the genesis of microRNAs. *Nature* **432**, 235–240.
- Gromak, N., Dienstbier, M., Macias, S., Plass, M., Eyra, E., Cáceres, J.F., and Proudfoot, N.J. (2013). Drosha regulates gene expression independently of RNA cleavage function. *Cell Rep.* **5**, 1499–1510.
- Gu, W., Shirayama, M., Conte, D., Jr., Vasale, J., Batista, P.J., Claycomb, J.M., Moresco, J.J., Youngman, E.M., Keys, J., Stoltz, M.J., et al. (2009). Distinct argonaute-mediated 22G-RNA pathways direct genome surveillance in the *C. elegans* germline. *Mol. Cell* **36**, 231–244.
- Ha, M., and Kim, V.N. (2014). Regulation of microRNA biogenesis. *Nat. Rev. Mol. Cell Biol.* **15**, 509–524.
- Han, J., Lee, Y., Yeom, K.H., Kim, Y.K., Jin, H., and Kim, V.N. (2004). The Drosha-DGCR8 complex in primary microRNA processing. *Genes Dev.* **18**, 3016–3027.
- Han, J., Lee, Y., Yeom, K.H., Nam, J.W., Heo, I., Rhee, J.K., Sohn, S.Y., Cho, Y., Zhang, B.T., and Kim, V.N. (2006). Molecular basis for the recognition of primary microRNAs by the Drosha-DGCR8 complex. *Cell* **125**, 887–901.
- Jeronimo, C., Collin, P., and Robert, F. (2016). The RNA Polymerase II CTD: the increasing complexity of a low-complexity protein domain. *J. Mol. Biol.* **428**, 2607–2622.
- Kim, Y.K., and Kim, V.N. (2007). Processing of intronic microRNAs. *EMBO J.* **26**, 775–783.
- Kim, M., Krogan, N.J., Vasiljeva, L., Rando, O.J., Nedeá, E., Greenblatt, J.F., and Buratowski, S. (2004). The yeast Rat1 exonuclease promotes transcription termination by RNA polymerase II. *Nature* **432**, 517–522.
- Kwon, S.C., Nguyen, T.A., Choi, Y.G., Jo, M.H., Hohng, S., Kim, V.N., and Woo, J.S. (2016). Structure of Human DROSHA. *Cell* **164**, 81–90.
- Landthaler, M., Yalcin, A., and Tuschl, T. (2004). The human DiGeorge syndrome critical region gene 8 and its D. melanogaster homolog are required for miRNA biogenesis. *Curr. Biol.* **14**, 2162–2167.
- Lee, Y., Ahn, C., Han, J., Choi, H., Kim, J., Yim, J., Lee, J., Provost, P., Rådmark, O., Kim, S., and Kim, V.N. (2003). The nuclear RNase III Drosha initiates microRNA processing. *Nature* **425**, 415–419.
- Lee, Y., Kim, M., Han, J., Yeom, K.H., Lee, S., Baek, S.H., and Kim, V.N. (2004). MicroRNA genes are transcribed by RNA polymerase II. *EMBO J.* **23**, 4051–4060.
- Lee, Y.S., Pressman, S., Address, A.P., Kim, K., White, J.L., Cassidy, J.J., Li, X., Lubell, K., Lim, D.H., Cho, I.S., et al. (2009). Silencing by small RNAs is linked to endosomal trafficking. *Nat. Cell Biol.* **11**, 1150–1156.
- Ma, H., Wu, Y., Choi, J.G., and Wu, H. (2013). Lower and upper stem-single-stranded RNA junctions together determine the Drosha cleavage site. *Proc. Natl. Acad. Sci. U S A* **110**, 20687–20692.
- Macias, M.J., Wiesner, S., and Sudol, M. (2002). WW and SH3 domains, two different scaffolds to recognize proline-rich ligands. *FEBS Lett.* **513**, 30–37.
- Maroney, P.A., Chamnongpol, S., Souret, F., and Nilsen, T.W. (2007). A rapid, quantitative assay for direct detection of microRNAs and other small RNAs using splinted ligation. *RNA* **13**, 930–936.
- Morlando, M., Ballarino, M., Gromak, N., Pagano, F., Bozzoni, I., and Proudfoot, N.J. (2008). Primary microRNA transcripts are processed co-transcriptionally. *Nat. Struct. Mol. Biol.* **15**, 902–909.
- Morris, D.P., Phatnani, H.P., and Greenleaf, A.L. (1999). Phospho-carboxyl-terminal domain binding and the role of a prolyl isomerase in pre-mRNA 3'-End formation. *J. Biol. Chem.* **274**, 31583–31587.
- Naftelberg, S., Schor, I.E., Ast, G., and Kornblihtt, A.R. (2015). Regulation of alternative splicing through coupling with transcription and chromatin structure. *Annu. Rev. Biochem.* **84**, 165–198.
- Nguyen, T.A., Jo, M.H., Choi, Y.G., Park, J., Kwon, S.C., Hohng, S., Kim, V.N., and Woo, J.S. (2015). Functional anatomy of the human Microprocessor. *Cell* **161**, 1374–1387.
- Ni, Z., Schwartz, B.E., Werner, J., Suarez, J.R., and Lis, J.T. (2004). Coordination of transcription, RNA processing, and surveillance by P-TEFb kinase on heat shock genes. *Mol. Cell* **13**, 55–65.
- Nojima, T., Gomes, T., Grosso, A.R., Kimura, H., Dye, M.J., Dhir, S., Carmo-Fonseca, M., and Proudfoot, N.J. (2015). Mammalian NET-seq reveals genome-wide nascent transcription coupled to RNA processing. *Cell* **161**, 526–540.
- Olive, V., Sabio, E., Bennett, M.J., De Jong, C.S., Biton, A., McGann, J.C., Greaney, S.K., Sodik, N.M., Zhou, A.Y., Balakrishnan, A., et al. (2013). A component of the mir-17-92 polycistronic oncomir promotes oncogene-dependent apoptosis. *eLife* **2**, e00822.
- Patton, J.S., Gomes, X.V., and Geyer, P.K. (1992). Position-independent germline transformation in *Drosophila* using a cuticle pigmentation gene as a selectable marker. *Nucleic Acids Res.* **20**, 5859–5860.
- Pawlicki, J.M., and Steitz, J.A. (2008). Primary microRNA transcript retention at sites of transcription leads to enhanced microRNA production. *J. Cell Biol.* **182**, 61–76.
- Pfeffer, S., Zavolan, M., Grässer, F.A., Chien, M., Russo, J.J., Ju, J., John, B., Enright, A.J., Marks, D., Sander, C., and Tuschl, T. (2004). Identification of virus-encoded microRNAs. *Science* **304**, 734–736.
- Pressman, S., Reinke, C.A., Wang, X., and Carthew, R.W. (2012). A systematic genetic screen to dissect the microRNA pathway in *Drosophila*. *G3 (Bethesda)* **2**, 437–448.
- Price, D.H. (2000). P-TEFb, a cyclin-dependent kinase controlling elongation by RNA polymerase II. *Mol. Cell Biol.* **20**, 2629–2634.
- Quick-Cleveland, J., Jacob, J.P., Weitz, S.H., Shoffner, G., Senturia, R., and Guo, F. (2014). The DGCR8 RNA-binding heme domain recognizes primary microRNAs by clamping the hairpin. *Cell Rep.* **7**, 1994–2005.
- Ryazansky, S.S., Gvozdev, V.A., and Berezikov, E. (2011). Evidence for post-transcriptional regulation of clustered microRNAs in *Drosophila*. *BMC Genomics* **12**, 371.
- Schröder, S., Herker, E., Itzen, F., He, D., Thomas, S., Gilchrist, D.A., Kaehlecke, K., Cho, S., Pollard, K.S., Capra, J.A., et al. (2013). Acetylation of RNA

- polymerase II regulates growth-factor-induced gene transcription in mammalian cells. *Mol. Cell* 52, 314–324.
- Schwartz, B.E., Larochelle, S., Suter, B., and Lis, J.T. (2003). Cdk7 is required for full activation of *Drosophila* heat shock genes and RNA polymerase II phosphorylation in vivo. *Mol. Cell. Biol.* 23, 6876–6886.
- Scotto-Lavino, E., Du, G., and Frohman, M.A. (2006). Amplification of 5' end cDNA with 'new RACE'. *Nat. Protoc.* 1, 3056–3061.
- Shirayama, M., Seth, M., Lee, H.C., Gu, W., Ishidate, T., Conte, D., Jr., and Mello, C.C. (2012). piRNAs initiate an epigenetic memory of nonself RNA in the *C. elegans* germline. *Cell* 150, 65–77.
- Sun, K., Jee, D., de Navas, L.F., Duan, H., and Lai, E.C. (2015). Multiple in vivo biological processes are mediated by functionally redundant activities of *Drosophila* mir-279 and mir-996. *PLoS Genet.* 11, e1005245.
- Suzuki, H.I., Young, R.A., and Sharp, P.A. (2017). Super-enhancer-mediated RNA processing revealed by integrative microRNA network analysis. *Cell* 168, 1000–1014.e1015.
- Truscott, M., Islam, A.B.M.M.K., López-Bigas, N., and Frolov, M.V. (2011). mir-11 limits the proapoptotic function of its host gene, dE2f1. *Genes Dev.* 25, 1820–1834.
- Truscott, M., Islam, A.B.M.M.K., Lightfoot, J., López-Bigas, N., and Frolov, M.V. (2014). An intronic microRNA links Rb/E2F and EGFR signaling. *PLoS Genet.* 10, e1004493.
- Van Wynsberghe, P.M., Kai, Z.S., Massirer, K.B., Burton, V.H., Yeo, G.W., and Pasquinelli, A.E. (2011). LIN-28 co-transcriptionally binds primary let-7 to regulate miRNA maturation in *Caenorhabditis elegans*. *Nat. Struct. Mol. Biol.* 18, 302–308.
- Verdecia, M.A., Bowman, M.E., Lu, K.P., Hunter, T., and Noel, J.P. (2000). Structural basis for phosphoserine-proline recognition by group IV WW domains. *Nat. Struct. Biol.* 7, 639–643.
- Weitz, S.H., Gong, M., Barr, I., Weiss, S., and Guo, F. (2014). Processing of microRNA primary transcripts requires heme in mammalian cells. *Proc. Natl. Acad. Sci. U S A* 111, 1861–1866.
- Yin, S., Yu, Y., and Reed, R. (2015). Primary microRNA processing is functionally coupled to RNAP II transcription in vitro. *Sci. Rep.* 5, 11992.
- Yu, J., Wang, F., Yang, G.-H., Wang, F.-L., Ma, Y.-N., Du, Z.-W., and Zhang, J.-W. (2006). Human microRNA clusters: genomic organization and expression profile in leukemia cell lines. *Biochem. Biophys. Res. Commun.* 349, 59–68.
- Zeng, Y., and Cullen, B.R. (2003). Sequence requirements for micro RNA processing and function in human cells. *RNA* 9, 112–123.